Journal of Applied Analysis and Computation
Volume 16, Number 5, October 2026, 2264–2286
Website:http://www.jaac-online.com
DOI:10.11948/20250191

EXPLORING SOLITON FAMILIES IN β FRACTIONAL COUPLED NLSES WITH VARIABLE COEFFICIENTS USING IMPROVED MODIFIED EXTENDED TANH-FUNCTION METHOD*

Ahmed Ramady[1,2], Hamdy M. Ahmed[3,†], Khadiga A. Ismail[4] and Wafaa B. Rabie[5]

Abstract This research presents a groundbreaking analytical investigation of optical soliton dynamics within the framework of variable-coefficient coupled higher-order nonlinear Schrödinger equation (NLSE) incorporating β-fractional derivatives. The study introduces a novel application of the improved modified extended tanh-function (IMETF) method to derive exact analytical solutions that capture the complex interplay between fractional derivatives, variable coefficients, and higher-order nonlinear effects. Our methodology enables the systematic transformation of the intricate fractional NLSE system into mathematically tractable forms, yielding an unprecedented spectrum of soliton solutions including bright, dark, singular, periodic, Jacobi elliptic, rational, and hyperbolic wave structures. The incorporation of β-fractional derivatives introduces fundamentally new propagation characteristics and non-local effects that significantly enhance soliton controllability and stability. Through comprehensive numerical simulations and graphical analysis, we demonstrate how fractional-order parameters and variable coefficients collectively govern soliton dynamics, enabling precise manipulation of wave properties in inhomogeneous media. This work makes substantial contributions to both theoretical and applied nonlinear optics by establishing a robust analytical framework for solving complex fractional NLSE systems, revealing novel soliton behaviors with enhanced stability properties, and providing practical insights for advanced applications in optical communications, photonic device engineering, and nonlinear wave control technologies. The results demonstrate the IMETF method's exceptional capability in addressing challenging nonlinear wave phenomena while opening new avenues for soliton manipulation in fractional-order systems with variable parameters.

Keywords Variable-coefficient coupled higher-order NLS equation, nonlinear wave propagation, fractional calculus.

MSC(2010) 35G20, 35C07, 35C08, 35C09.

[†]The corresponding author.
[1]GRC Department, The Applied College, King Abdulaziz University, Jeddah 21589, Saudi Arabia
[2]Department of Mathematics and Computer Science, Faculty of Science, Beni-Suef University, Beni-Suef, Egypt
[3]Department of Physics and Engineering Mathematics, Higher Institute of Engineering, El Shorouk Academy, Cairo, Egypt
[4]Department of Clinical Laboratory Sciences, College of Applied Medical Sciences, Taif University, Taif 21944, Saudi Arabia
[5]Department of Mathematics, Faculty of Science, Luxor University, Taiba, Luxor, Egypt
*The authors would like to acknowledge the Deanship of Graduate Studies and Scientific Research, Taif University for funding this work.
Email: anasr@kau.edu.sa(A. Ramady), hamdy_17eg@yahoo.com(H. M. Ahmed), khadigaah.aa@tu.edu.sa(K. A. Ismail), wbr_allah_raby @yahoo.com(W. B. Rabie)

1. Introduction

The study of optical solitons has transcended traditional boundaries, especially in the realm of nonlinear optics and photonics, where they serve not only as fundamental wave packets but also as carrier signals in advanced communication systems [3, 7]. Optical solitons are distinct wave phenomena noted for their capacity to preserve their form despite traveling through a nonlinear medium. Numerous studies have contributed to important improvements in nonlinear optics, strengthening our understanding of light transmission in optical fibers, which is crucial for modern optical communications [5, 6, 18]. The dynamics of optical solitons are akin to particle interactions, allowing researchers to explore fundamental physical phenomena by studying these interactions [14]. Solitons have distinctive characteristics, including self-focusing and elasticity during collisions, underscoring the relationship between particle-like behavior and wave events [15]. In recent years, the exploration of variable-coefficient coupled higher-order nonlinear Schrödinger equations has gained prominence due to their ability to model complex physical phenomena more accurately than their constant-coefficient counterparts [13,21,32]. The variable-coefficient coupled higher-order nonlinear Schrödinger equation (VCHNLSE) is a key extension of the classical nonlinear Schrödinger equation, accounting for variations in medium characteristics that affect soliton propagation. Its development is closely linked to progress in nonlinear optics, fluid mechanics, and mathematical physics. Research on classical Coupled Nonlinear Schrödinger (CNLS) equations began in the 1970s, notably with the 1974 introduction of the Manakov system, which featured uniform nonlinear interactions among multiple components. This system laid the groundwork for investigating soliton dynamics in nonlinear optics [11]. As optical communication technologies evolved, there arose the need to consider variable coefficients in the NLSE framework, leading to the formulation of the Variable Coefficient Nonlinear Schrödinger Equations (VCNLS). This adaptation is crucial for accurately modeling realistic scenarios in various media, such as optical fibers, where properties like the refractive index can change over time and space [20]. Complementary research has expanded our understanding through investigations of stochastic effects, numerical methods, and diverse physical applications. Significant contributions include the analysis of white noise impacts on optical solitons in stochastic fourth-order nonlinear Schrödinger equations [29], the development of cubic spline methods for boundary value problems in complex systems [19], studies of beta-time fractional biological population models with abundant solitary wave structures [23], investigations of nonlinear pulse propagation in monomode optical fibers using Fokas systems [30], and examinations of heat conduction dynamics through Lie symmetry and modulation instability analysis [10]. These works collectively advance our capability to model and understand complex nonlinear phenomena across multiple physical domains. Recent advancements in fractional calculus have further enriched this field, demonstrating enhanced modeling capabilities for complex nonlinear systems with memory effects and long-range interactions. Various analytical methods have been successfully applied to fractional nonlinear models, revealing new insights into soliton dynamics, wave propagation, and chaotic behavior in diverse physical contexts, including optical systems, ferromagnetic materials, and fluid dynamics [4, 8, 9, 26, 27]. Researchers have utilized several mathematical methods, including the improved modified extended tanh function method [1, 16, 25], Extended and modified rational expansion method [22], Extended F-expansion method [24], Laplace-Adomian decomposition method [12], Sardar's Sub-Equation Approach [17], the modified extended direct algebraic method [2], and others, to reach accurate solutions for many communication systems and other systems.

This paper studies the variable-coefficient coupled higher-order nonlinear Schrödinger equa-

tion (NLSE), an advanced mathematical model used to study nonlinear wave phenomena. Recent work has shown that incorporating variable coefficients facilitates the study of soliton solutions with controllable dynamics, allowing for better manipulation of soliton propagation relevant to practical applications in telecommunications and material science. While significant progress has been made in studying fractional NLSE models, most previous research has focused on simplified models with constant coefficients or lower-order interactions. This study introduces a substantial advancement beyond the current state-of-the-art by uniquely integrating three critical aspects: A coupled higher-order model describing the interaction of two wave modes, time-dependent variable coefficients for more realistic simulation of non-uniform media and dynamic control, and the application of β-fractional derivatives that provide superior mathematical precision for describing systems with memory and non-local effects. This multi-dimensional integration enables the investigation of more complex nonlinear phenomena that have been insufficiently explored in the existing literature. To achieve this, we apply the Improved Modified Extended Tanh-Function (IMETF) method for the first time to the proposed system of variable-coefficient coupled higher-order NLSEs with β-fractional derivatives. This powerful analytical technique enables us to derive a broader and richer set of exact analytical solutions, including new types of dark, bright, and singular soliton solutions previously unreported for this specific model, alongside singular periodic solutions, Jacobi elliptic function solutions, rational solutions, and exponential solutions. Furthermore, we provide a graphical analysis that clearly illustrates the pronounced effect of the fractional derivative (β) on the dynamics and properties of these solutions, offering new qualitative insights. The historical development of the nonlinear Schrödinger equation provides important context for understanding the novelty of our model. The standard nonlinear Schrödinger equation (NLSE) was first derived in the 1970s to describe pulse propagation in optical fibers, with Hasegawa and Tappert's seminal work demonstrating its soliton solutions. Subsequent developments introduced coupled NLSE systems to model interactions between multiple optical fields, notably the Manakov system for polarization-multiplexed transmission. The incorporation of higher-order terms emerged as a crucial advancement to account for additional physical effects, including third-order dispersion, self-steepening, and stimulated Raman scattering, particularly relevant for ultrashort pulses. Meanwhile, variable-coefficient formulations were developed to model realistic inhomogeneous media where parameters such as dispersion and nonlinearity vary along the propagation distance. More recently, fractional calculus has been introduced into nonlinear wave equations to capture nonlocal effects and memory properties that cannot be described by integer-order derivatives. However, the integration of all these features—coupled with higher-order nonlinearities, variable coefficients, and β - fractional derivatives—in a unified framework represents a significant advancement beyond previous models. This work seeks to identify numerous solitons and other solutions of the following variable-coefficient coupled higher-order NLSE with $\beta-$ fractional derivatives using the Improved Modified Extended Tanh-Function method [31]:

$$
\begin{aligned}
&i\,\frac{\partial^{\beta}\mathcal{P}}{\partial t^{\beta}}+\mathcal{P}_{\mathrm{xx}}+2\,\sigma\,\mathcal{P}\left(|\mathcal{P}|^{2}+2\,|\mathcal{U}|^{2}\right)+2\,\sigma\,\mathcal{P}^{*}\,\mathcal{U}^{2}+i\,\varepsilon(t)\,\mathcal{P}_{\mathrm{xxx}}\\
&+6\,i\,\sigma\,\varepsilon(t)\,\mathcal{P}_{x}\left(|\mathcal{P}|^{2}+|\mathcal{U}|^{2}\right)+6\,i\,\sigma\,\varepsilon(t)\,\mathcal{U}_{x}\,\left(\mathcal{P}^{*}\,\mathcal{U}+\mathcal{P}\,\mathcal{U}^{*}\right)=0, \qquad (1.1)\\
&i\,\frac{\partial^{\beta}\mathcal{U}}{\partial t^{\beta}}+\mathcal{U}_{\mathrm{xx}}+2\,\sigma\,\mathcal{U}\left(|\mathcal{U}|^{2}+2\,|\mathcal{P}|^{2}\right)+2\,\sigma\,\mathcal{U}^{*}\,\mathcal{P}^{2}+i\,\varepsilon(t)\,\mathcal{U}_{\mathrm{xxx}}\\
&+6\,i\,\sigma\,\varepsilon(t)\,\mathcal{U}_{x}\left(|\mathcal{U}|^{2}+|\mathcal{P}|^{2}\right)+6\,i\,\sigma\,\varepsilon(t)\,\mathcal{P}_{x}\,\left(\mathcal{U}^{*}\,\mathcal{P}+\mathcal{U}\,\mathcal{P}^{*}\right)=0. \qquad (1.2)
\end{aligned}
$$

The $\beta-$ derivative of the function $\mathcal{P}(x,t)$ at the specified order β is defined as follows [2]:

$$\frac{\partial^{\beta}\mathcal{P}(x,t)}{\partial t^{\beta}} = \lim_{h\to 0}\frac{1}{h}\left[\mathcal{P}\left(x, t\ + h\left[\frac{1}{\Gamma(\beta)}+t\right]^{1-\beta}\right) - \mathcal{P}(x,t)\right], \quad \forall\ t>0,\ \beta\in(0,1]. \tag{1.3}$$

In this context, $\mathcal{P}$ and $\mathcal{U}$ denote the wave functions of two interacting modes, while σ is a constant, and $\varepsilon(t)$ is a time-dependent coefficient associated.

The improved modified extended tanh-function (IMETF) method is an efficient analytical instrument employed to investigate isolated waves and microwave solutions in diverse scientific domains. It applies to many types of nonlinear partial differential equations (PDEs). A comparative analysis reveals distinct advantages of the IMETF method over other analytical approaches for solving β-fractional NLSEs. Unlike the Hirota bilinear method, which requires specific bilinear forms that can be challenging for complex fractional systems, the IMETF method offers direct applicability to variable-coefficient fractional equations without complex transformations. Compared to the Exp-function method that often yields solutions in complex exponential forms, the IMETF provides solutions in more physically intuitive forms (hyperbolic, trigonometric, rational) while maintaining mathematical rigor. Furthermore, while the (G'/G)-expansion method typically produces limited solution varieties, the IMETF method generates a wider spectrum of solutions including bright, dark, singular solitons, and periodic solutions from a unified framework. The computational efficiency of IMETF in systematically reducing partial differential equations to algebraic systems without extensive symbolic manipulation makes it particularly suitable for our complex system with β-fractional derivatives and variable coefficients. In this study, the application of the IMETF method to this sophisticated system yields a wide spectrum of solutions. These include novel dark, bright, and singular soliton solutions, singular periodic solutions, Jacobi elliptic function solutions, rational solutions, and exponential solutions. Graphical representations of selected solutions are provided, accompanied by a detailed explanation of the influential role played by the fractional derivative parameter. These results highlight the method's effectiveness and robustness.

This is how this article is organized: Section 2 provides an overview of the improved modified extended tanh-function (IMETF) method. Section 3 investigates solitons and other solutions to the proposed system using Wolfram Mathematica for symbolic computations. Section 4 presents physical applications of solitons in variable-coefficient nonlinear Schrödinger equations with β-fractional derivatives through graphical representations. Section 5 discusses the results and their implications. The main findings are summarized in Section 6, and future research directions are outlined in Section 7.

2. Overview of the improved modified extended tanh-function method

This section presents a detailed overview of the extended direct algebraic method, emphasizing its key components and significance in enhancing understanding of this mathematical approach. This method offers a systematic framework for solving partial differential equations (PDEs), providing insights into its application and effectiveness. We will examine the detailed NPDE below and demonstrate the procedures and techniques for implementing the improved modified extended tanh-function (IMETF) method, assuming the NPDE is as follows [16]:

$$\mathcal{R}\left(\mathcal{U}, \frac{\partial\mathcal{U}(x,t)}{\partial x}, \frac{\partial^{\beta}\mathcal{U}(x,t)}{\partial t^{\beta}}, \frac{\partial^{2}\mathcal{U}(x,t)}{\partial x^{2}}, \ldots\right) = 0, \tag{2.1}$$

the polynomial $\mathcal{R}$ is made up of $\mathcal{U}(x,t)$ and its partial derivatives with respect to time t and the dynamic system's spatial dimension x.

To solve the above equation, we follow the following procedures:

Procedure-(1): We use the following assumption:

$$\mathcal{U}(x,t) = \mathcal{P}(\eta); \quad \eta = \mathcal{T}\ x + \frac{\mathcal{L}}{\beta}\ \left(\frac{1}{\Gamma(\beta)} + t\right)^{\beta}, \tag{2.2}$$

where the real-valued constants $\mathcal{T}$ and $\mathcal{L}$ are used. $\mathcal{P}(\eta)$ acts as a function of the resulting solution.

The partial derivatives in Eq. (2.2) are substituted by the transformations given in Eq. (2.1) to convert it to the subsequent nonlinear ordinary differential system:

$$\mathcal{E}(\mathcal{P},\ \mathcal{P}',\ \mathcal{P}'',\ \mathcal{P}''',\ \ldots\ldots) = 0. \tag{2.3}$$

Procedure-(2): To solve Eq. (2.3) using the applied method, the following solution series is applied:

$$\mathcal{P}(\eta) = \alpha_0 + \sum_{i=1}^{\mathbb{N}} \left[\alpha_i\ \mathcal{U}^i(\eta) + B_i\ \mathcal{U}^{-i}(\eta)\right], \tag{2.4}$$

where $\alpha_0,\ \alpha_i$, and $B_i\ (i = 1, 2, 3, ...)$ are real constants that are calculated under the constraint $\alpha_N^2 + B_{-N}^2 \neq 0$.

Procedure-(3): To determine the balancing constant $\mathbb{N}$, we apply the balance rule between the nonlinearity and dispersion in Eq. (2.3), while also considering the following constraint for:

$$\mathcal{U}'(\eta) = \epsilon\sqrt{d_0 + d_1\ \mathcal{U}(\eta) + d_2\ \ \mathcal{U}(\eta)^2 + d_3\mathcal{U}(\eta)^3 + d_4\ \mathcal{U}(\eta)^4}, \tag{2.5}$$

where $\epsilon = \pm 1$ and $d_j\ (j = 0, 1, 2, 3, 4)$ are real valued constants. Various fundamental solutions are derived from Eq. (2.4) by exploring different possible values of d_j.

From the different possible values of d_0, d_1, d_2, d_3 and d_4, from Eq. (2.5) the various kinds of fundamental solutions can be obtained as follows:

Case 1. $d_0 = d_1 = d_3 = 0$.

A bell-shaped solitary wave solution, a triangular type solution and a rational solution are obtained:

$$\mathcal{U}(\eta) = \sqrt{-\frac{d_2}{d_4}}\,\mathrm{sech}(\sqrt{d_2}\ \eta), \qquad d_2 > 0, d_4 < 0,$$

$$\mathcal{U}(\eta) = \sqrt{-\frac{d_2}{d_4}}\,\sec(\sqrt{-d_2}\ \eta), \qquad d_2 < 0, d_4 > 0,$$

$$\mathcal{U}(\eta) = \frac{-\varepsilon}{\sqrt{d_4}\ \eta}, \qquad d_2 = 0, d_4 > 0.$$

Case 2. $d_1 = d_3 = 0$.

A kink-shaped solitary wave solution, a triangular type solution and three Jacobi elliptic function type solutions are obtained:

$$\mathcal{U}(\eta) = \varepsilon\sqrt{-\frac{d_2}{2d_4}}\tanh\left(\sqrt{-\frac{d_2}{2}}\ \eta\right), \qquad d_2 < 0, d_4 > 0, d_0 = \frac{d_2^2}{4d_4},$$

$$\mathcal{U}(\eta)=\varepsilon\sqrt{\frac{d_2}{2d_4}}\tan\left(\sqrt{\frac{d_2}{2}}\ \eta\right),\qquad d_2>0,\,d_4>0,\,d_0=\frac{d_2^2}{4d_4},$$

$$\mathcal{U}(\eta)=\sqrt{\frac{-d_2m^2}{d_4(2m^2-1)}}\,\mathrm{cn}\left(\sqrt{\frac{d_2}{2m^2-1}}\ \eta\right),\qquad d_2>0,\,d_4<0,\,d_0=\frac{d_2^2m^2(1-m^2)}{d_4(2m^2-1)^2},$$

$$\mathcal{U}(\eta)=\sqrt{\frac{-m^2}{d_4(2-m^2)}}\,\mathrm{dn}\left(\sqrt{\frac{d_2}{2-m^2}}\ \eta\right),\qquad d_2>0,\,d_4<0,\,d_0=\frac{d_2^2(1-m^2)}{d_4(2-m^2)^2},$$

$$\mathcal{U}(\eta)=\varepsilon\sqrt{-\frac{d_2m^2}{d_4(1+m^2)}}\,\mathrm{sn}\left(\sqrt{-\frac{d_2}{1+m^2}}\ \eta\right),\qquad d_2<0,\,d_4>0,\,d_0=\frac{d_2^2m^2}{d_4(m^2+1)^2},$$

where m is the modulus of the Jacobi elliptic functions.

Case 3. $d_3=d_4=0$.

An exponential type solution, two triangular type solutions and two hyperbolic type solutions are obtained:

$$\mathcal{U}(\eta)=-\frac{d_1}{2d_2}+\exp(\varepsilon\sqrt{d_2}\ \eta),\qquad d_2>0,\,d_0=\frac{d_1^2}{4d_2},$$

$$\mathcal{U}(\eta)=-\frac{d_1}{2d_2}+\frac{\varepsilon\,d_1}{2d_2}\sin(\sqrt{-d_2}\ \eta),\qquad d_0=0,\,d_2<0,$$

$$\mathcal{U}(\eta)=-\frac{d_1}{2d_2}+\frac{\varepsilon\,d_1}{2d_2}\sinh(2\sqrt{d_2}\ \eta),\qquad d_0=0,\,d_2>0,$$

$$\mathcal{U}(\eta)=\varepsilon\sqrt{-\frac{d_0}{d_2}}\sin(\sqrt{-d_2}\ \eta),\qquad d_1=0,\,d_0>0,\,d_2<0,$$

$$\mathcal{U}(\eta)=\varepsilon\sqrt{\frac{d_0}{d_2}}\sinh(\sqrt{d_2}\ \eta),\qquad d_1=0,\,d_0>0,\,d_2>0.$$

Procedure-(4): A polynomial in $\mathcal{U}$ is derived by replacing Eqs. (2.4) and (2.5) into Eq. (2.3). Setting the sum of terms with identical powers to zero is the next step. Mathematica software will be used to solve the resulting system of nonlinear equations and ascertain the values of the unknowns. Novel soliton solutions for the suggested system are produced by this method.

3. Investigate solitons and other solutions to the proposed system

The selection of an appropriate wave transformation is crucial for successfully reducing a partial differential equation (PDE) system to an ordinary differential equation (ODE). Suppose the transformation used in this study to Eqs. (1.1) and (1.2) can be expressed in the following manner:

$$\mathcal{P}=\mathcal{R}_1(\eta)\ e^{i\mathcal{Q}},\tag{3.1}$$

$$\mathcal{U}=\mathcal{R}_2(\eta)\ e^{i\mathcal{Q}},\tag{3.2}$$

where

$$\eta=\mathcal{T}\ x+\frac{\mathcal{L}}{\beta}\ \left(\frac{1}{\Gamma(\beta)}+t\right)^{\beta},\qquad \&\qquad \mathcal{Q}=\gamma\ x+\frac{w}{\beta}\ \left(\frac{1}{\Gamma(\beta)}+t\right)^{\beta}+\Phi.\tag{3.3}$$

The amplitude components are denoted by $\mathcal{R}_i(\eta)$ (for $i = 1, 2$), with γ representing the soliton frequency, w the wave number, and Φ the phase constant. The normalized wave vector and frequency are represented by the parameters $\mathcal{T}$ and $\mathcal{L}$, respectively. The parameter constraints that emerge during the solution process are not arbitrary but represent essential *compatibility conditions* for the existence of non-trivial solutions. These constraints, typically appearing as algebraic relations between $\mathcal{T}$, $\mathcal{L}$, γ, and w, define the specific dispersion relations that must be satisfied for sustained wave propagation in the nonlinear medium. They ensure the mathematical consistency of the reduced ODE system and have direct physical interpretations in terms of energy conservation and phase-matching conditions.

Nonlinear ordinary differential equations (NLODEs) are produced by applying the previously indicated wave transformations to Eqs. (1.1) and (1.2). These NLODEs are separated into their real and imaginary components as follows:

$$\begin{aligned}&\mathcal{T}^2[1-3\gamma\ \varepsilon(t)]\ \mathcal{R}_j'' + 6\ \sigma\ [1-3\ \gamma\ \varepsilon(t)]\ \mathcal{R}_j\ \mathcal{R}_{\tilde{j}}^2 + 2\ \sigma\ [1-3\gamma\ \varepsilon(t)]\ \mathcal{R}_j^3\\ &-\left[\gamma^2-\gamma^3\ \varepsilon(t)+w\right]\ \mathcal{R}_j = 0, \end{aligned} \tag{3.4}$$

$$\begin{aligned}&\mathcal{T}^3\ \varepsilon(t)\ \mathcal{R}_j^{(3)} + 6\ \sigma\ \mathcal{T}\ \varepsilon(t)\mathcal{R}_{\tilde{j}}^2\ \mathcal{R}_j' + 12\ \sigma\ \mathcal{T}\ \varepsilon(t)\ \mathcal{R}_j\mathcal{R}_{\tilde{j}}\mathcal{R}_{\tilde{j}}' + 6\ \sigma\ \mathcal{T}\ \varepsilon(t)\ \mathcal{R}_j^2\ \mathcal{R}_j'\\ &+\left[-3\ \mathcal{T}\ \gamma^2\ \varepsilon(t)+2\ \gamma\ \mathcal{T}+\mathcal{L}\right]\ \mathcal{R}_j' = 0, \end{aligned} \tag{3.5}$$

where $\tilde{j} = 3 - j$ and $j = 1, 2$. The balancing principle yields the following results:

$$\mathcal{R}_{\tilde{j}} = h\ \mathcal{R}_j, \tag{3.6}$$

where h is a constant that satisfies $h \neq 0$ and $h \neq 1$.

This results in a transformation of Eqs. (3.4) and (3.5) into the following:

$$\mathcal{T}^2[1-3\gamma\ \varepsilon(t)]\ \mathcal{R}_j'' + 2\ \sigma\left[1+3\ h^2\right][1-3\ \gamma\ \varepsilon(t)]\ \mathcal{R}_j^3 - \left[\gamma^2-\gamma^3\ \varepsilon(t)+w\right]\ \mathcal{R}_j = 0, \tag{3.7}$$

$$\mathcal{T}^3\ \varepsilon(t)\ \mathcal{R}_j^{(3)} + 6\ \left[1+3\ h^2\right]\ \sigma\ \mathcal{T}\ \varepsilon(t)\ \mathcal{R}_j^2\ \mathcal{R}_j' + \left[-3\ \mathcal{T}\ \gamma^2\ \varepsilon(t)+2\ \gamma\ \mathcal{T}+\mathcal{L}\right]\ \mathcal{R}_j' = 0. \tag{3.8}$$

The following is the reformulation of Eq. (3.8) using Eq. (3.8):

$$\begin{aligned}&\mathcal{T}^3\ \varepsilon(t)\ \mathcal{R}_j\ \mathcal{R}_j^{(3)} - 3\ \mathcal{T}^3\ \varepsilon(t)\ \mathcal{R}_j'\ \mathcal{R}_j''\\ &+\left[3\ r\ \gamma^3\ \mathcal{T}\ \varepsilon(t)^2 - 3\ \mathcal{T}\ \varepsilon(t)\left[\gamma^2+r\ \left(\gamma^2+w\right)\right] + 2\ \gamma\ \mathcal{T}+\mathcal{L}\right]\ \mathcal{R}_j\ \mathcal{R}_j' = 0, \end{aligned} \tag{3.9}$$

where $r = \frac{1}{3\ \gamma\ \varepsilon(t)-1}$.

The second section explains how to generate exact solutions for Eq. (3.8) as follows:

$$\mathcal{R}_j = \alpha_0 + \alpha_1\ \mathcal{U}(\eta) + \frac{B_1}{\mathcal{U}(\eta)}, \tag{3.10}$$

where the real constants α_0, α_1, and B_1 are determined by the restriction $\alpha_1^2 + B_1^2 \neq 0$.

We obtain a polynomial in $\mathcal{U}(\eta)$ by inserting Eq. (3.10) and the restriction from Eq. (2.5) into Eq. (3.9). When like terms are combined and set to zero, an algebraic system of non-linear equations is produced. After that, we solve these equations using Wolfram Mathematica to produce possible solutions for the suggested system, which fall into the following categories:

First Situation: If the limitations $d_0 = d_1 = 0,$ and $d_3 = 0$ are applied, we obtain a restricted set of solutions for the algebraic system, establishing a clear mathematical framework that yields limited results based on these conditions:

(1.1) $\alpha_1 = \alpha_1,\ \alpha_0 = B_1 = 0,\ \varepsilon(t) = \frac{2d_2\mathcal{T}^3+3\mathcal{T}\left(\gamma^2+r\left(\gamma^2+w\right)\right)\pm\sqrt{[2d_2\mathcal{T}^3+3\mathcal{T}(\gamma^2+r(\gamma^2+w))]^2-12\gamma^3r\mathcal{T}(2\gamma\mathcal{T}+\mathcal{L})}}{6\gamma^3r\mathcal{T}}$.

(1.2) $\alpha_0 = \alpha_1 = 0,\ B_1 = B_1,\ \varepsilon(t) = \frac{2d_2\mathcal{T}^3+3\mathcal{T}\left(\gamma^2+r\left(\gamma^2+w\right)\right)\pm\sqrt{[2d_2\mathcal{T}^3+3\mathcal{T}(\gamma^2+r(\gamma^2+w))]^2-12\gamma^3r\mathcal{T}(2\gamma\mathcal{T}+\mathcal{L})}}{6\gamma^3r\mathcal{T}}$.

We can now derive the exact solutions to Eqs. (1.1) and (1.2) based on the solutions from the set (1.1), which are outlined as follows:

(1.1.1) We obtain the bright soliton solutions as follows if $d_2 > 0$ and $d_4 < 0$ are satisfied:

$$\mathcal{P}_{1.1.1} = \alpha_1\sqrt{-\frac{d_2}{d_4}}\,\mathrm{sech}\left[\left(\mathcal{T}\ x+\frac{\mathcal{L}}{\beta}\ \left(\frac{1}{\Gamma(\beta)}+t\right)^{\beta}\right)\ \sqrt{d_2}\right]\ e^{i(\gamma\ x+\frac{w}{\beta}\ \left(\frac{1}{\Gamma(\beta)}+t\right)^{\beta}+\Phi)}, \tag{3.11}$$

$$\mathcal{U}_{1.1.1} = h\ \alpha_1\sqrt{-\frac{d_2}{d_4}}\,\mathrm{sech}\left[\left(\mathcal{T}\ x+\frac{\mathcal{L}}{\beta}\ \left(\frac{1}{\Gamma(\beta)}+t\right)^{\beta}\right)\ \sqrt{d_2}\right]\ e^{i(\gamma\ x+\frac{w}{\beta}\ \left(\frac{1}{\Gamma(\beta)}+t\right)^{\beta}+\Phi)}. \tag{3.12}$$

(1.1.2) We obtain the singular periodic solutions as follows if $d_2 < 0$ and $d_4 > 0$ are satisfied:

$$\mathcal{P}_{1.1.2} = \alpha_1\sqrt{-\frac{d_2}{d_4}}\,\mathrm{sec}\left[\left(\mathcal{T}\ x+\frac{\mathcal{L}}{\beta}\ \left(\frac{1}{\Gamma(\beta)}+t\right)^{\beta}\right)\ \sqrt{-d_2}\right]\ e^{i(\gamma\ x+\frac{w}{\beta}\ \left(\frac{1}{\Gamma(\beta)}+t\right)^{\beta}+\Phi)}, \tag{3.13}$$

$$\mathcal{U}_{1.1.2} = h\ \alpha_1\sqrt{-\frac{d_2}{d_4}}\,\mathrm{sec}\left[\left(\mathcal{T}\ x+\frac{\mathcal{L}}{\beta}\ \left(\frac{1}{\Gamma(\beta)}+t\right)^{\beta}\right)\ \sqrt{-d_2}\right]\ e^{i(\gamma\ x+\frac{w}{\beta}\ \left(\frac{1}{\Gamma(\beta)}+t\right)^{\beta}+\Phi)}. \tag{3.14}$$

(1.1.3) We obtain the rational solutions as follows if $d_2 = 0$ and $d_4 > 0$ are satisfied:

$$\mathcal{P}_{1.1.3} = \frac{\alpha_1}{\left[\mathcal{T}\ x+\frac{\mathcal{L}}{\beta}\ \left(\frac{1}{\Gamma(\beta)}+t\right)^{\beta}\right]\ \sqrt{d_4}}\ e^{i(\gamma\ x+\frac{w}{\beta}\ \left(\frac{1}{\Gamma(\beta)}+t\right)^{\beta}+\Phi)}, \tag{3.15}$$

$$\mathcal{U}_{1.1.3} = \frac{h\ \alpha_1}{(\mathcal{T}\ x+h\ t)\ \sqrt{d_4}}\ e^{i(\gamma\ x+\frac{w}{\beta}\ \left(\frac{1}{\Gamma(\beta)}+t\right)^{\beta}+\Phi)}. \tag{3.16}$$

We can now derive the exact solutions to Eqs. (1.1) and (1.2) based on the solutions from the set (1.2), which are outlined as follows:

(1.2.1) We obtain the hyperbolic solutions as follows if $d_2 > 0$ and $d_4 < 0$ are satisfied:

$$\mathcal{P}_{1.2.1} = B_1\ \sqrt{-\frac{d_4}{d_2}}\cosh\left[\left(\mathcal{T}\ x+\frac{\mathcal{L}}{\beta}\ \left(\frac{1}{\Gamma(\beta)}+t\right)^{\beta}\right)\ \sqrt{d_2}\right]\ e^{i(\gamma\ x+\frac{w}{\beta}\ \left(\frac{1}{\Gamma(\beta)}+t\right)^{\beta}+\Phi)}, \tag{3.17}$$

$$\mathcal{U}_{1.2.1} = h\ B_1\ \sqrt{-\frac{d_4}{d_2}}\cosh\left[\left(\mathcal{T}\ x+\frac{\mathcal{L}}{\beta}\ \left(\frac{1}{\Gamma(\beta)}+t\right)^{\beta}\right)\ \sqrt{d_2}\right]\ e^{i(\gamma\ x+\frac{w}{\beta}\ \left(\frac{1}{\Gamma(\beta)}+t\right)^{\beta}+\Phi)}. \tag{3.18}$$

(1.2.2) We obtain the periodic solutions as follows if $d_2 < 0$ and $d_4 > 0$ are satisfied:

$$\mathcal{P}_{1.2.2} = B_1\ \sqrt{-\frac{d_4}{d_2}}\cos\left[\left(\mathcal{T}\ x+\frac{\mathcal{L}}{\beta}\ \left(\frac{1}{\Gamma(\beta)}+t\right)^{\beta}\right)\ \sqrt{-d_2}\right]\ e^{i(\gamma\ x+\frac{w}{\beta}\ \left(\frac{1}{\Gamma(\beta)}+t\right)^{\beta}+\Phi)}, \tag{3.19}$$

$$\mathcal{U}_{1.2.2} = h\ B_1\ \sqrt{-\frac{d_4}{d_2}}\cos\left[\left(\mathcal{T}\ x + \frac{\mathcal{L}}{\beta}\ \left(\frac{1}{\Gamma(\beta)} + t\right)^{\beta}\right)\ \sqrt{-d_2}\right]\ e^{i(\gamma\ x + \frac{w}{\beta}\ \left(\frac{1}{\Gamma(\beta)}+t\right)^{\beta}+\Phi)}. \tag{3.20}$$

(1.2.3) We obtain the polynomial solutions as follows if $d_2 = 0$ and $d_4 > 0$ are satisfied:

$$\mathcal{P}_{1.2.3} = B_1\left(\mathcal{T}\ x + \frac{\mathcal{L}}{\beta}\ \left(\frac{1}{\Gamma(\beta)} + t\right)^{\beta}\right)\ \sqrt{d_4}\ e^{i(\gamma\ x + \frac{w}{\beta}\ \left(\frac{1}{\Gamma(\beta)}+t\right)^{\beta}+\Phi)}, \tag{3.21}$$

$$\mathcal{U}_{1.2.3} = h\ B_1\left(\mathcal{T}\ x + \frac{\mathcal{L}}{\beta}\ \left(\frac{1}{\Gamma(\beta)} + t\right)^{\beta}\right)\ \sqrt{d_4}\ e^{i(\gamma\ x + \frac{w}{\beta}\ \left(\frac{1}{\Gamma(\beta)}+t\right)^{\beta}+\Phi)}. \tag{3.22}$$

Second situation: If the limitations $d_1 = d_3 = d_6 = 0$ and $d_0 = \frac{d_2^2}{4d_4}$ are applied, we obtain a restricted set of solutions for the algebraic system, establishing a clear mathematical framework that yields limited results based on these conditions:

(2.1) $\alpha_0 = \alpha_1 = 0,\ B_1 = B_1,\ r = \frac{2\gamma\ \mathcal{T}+\mathcal{L}-\varepsilon(t)\left(2d_2\ \mathcal{T}^3+3\gamma^2\ \mathcal{T}\right)}{3\mathcal{T}\ \varepsilon(t)[\gamma^2-\gamma^3\ \varepsilon(t)+w]}$.

(3.2) $\alpha_0 = B_1 = 0,\ \alpha_1 = \alpha_1,\ r = \frac{2\gamma\ \mathcal{T}+\mathcal{L}-\varepsilon(t)\left(2d_2\ \mathcal{T}^3+3\gamma^2\ \mathcal{T}\right)}{3\mathcal{T}\ \varepsilon(t)[\gamma^2-\gamma^3\ \varepsilon(t)+w]}$.

(3.3) $\alpha_0 = 0,\ \alpha_1 = \frac{2B_1 d_4}{d_2},\ r = \frac{2\gamma\ \mathcal{T}+\mathcal{L}-\varepsilon(t)\left(2d_2\ \mathcal{T}^3-3\gamma^2\ \mathcal{T}\right)}{3\mathcal{T}\ \varepsilon(t)[\gamma^2-\gamma^3\ \varepsilon(t)+w]}$.

We can now obtain the exact solutions to Eqs. (1.1) and (1.2) based on the solution set (2.1), which is expressed as follows:

(2.1.1) The singular soliton solutions are obtained as follows if the following requirements are met $d_2 < 0$ and $d_4 > 0$:

$$\mathcal{P}_{2.1.1} = B_1\ \sqrt{-\frac{2\ d_4}{d_2}}\ \coth\left[\left(\mathcal{T}\ x + \frac{\mathcal{L}}{\beta}\ \left(\frac{1}{\Gamma(\beta)} + t\right)^{\beta}\right)\ \sqrt{-\frac{d_2}{2}}\right]\ e^{i(\gamma\ x + \frac{w}{\beta}\ \left(\frac{1}{\Gamma(\beta)}+t\right)^{\beta}+\Phi)}, \tag{3.23}$$

$$\mathcal{U}_{2.1.1} = h\ B_1\ \sqrt{-\frac{2\ d_4}{d_2}}\ \coth\left[\left(\mathcal{T}\ x + \frac{\mathcal{L}}{\beta}\ \left(\frac{1}{\Gamma(\beta)} + t\right)^{\beta}\right)\ \sqrt{-\frac{d_2}{2}}\right]\ e^{i(\gamma\ x + \frac{w}{\beta}\ \left(\frac{1}{\Gamma(\beta)}+t\right)^{\beta}+\Phi)}. \tag{3.24}$$

(2.1.2) The singular periodic solutions are obtained as follows if the following requirements are met $d_2 > 0$ and $d_4 > 0$:

$$\mathcal{P}_{2.1.2} = B_1\ \sqrt{\frac{2\ d_4}{d_2}}\ \cot\left[\left(\mathcal{T}\ x + \frac{\mathcal{L}}{\beta}\ \left(\frac{1}{\Gamma(\beta)} + t\right)^{\beta}\right)\ \sqrt{\frac{d_2}{2}}\right]\ e^{i(\gamma\ x + \frac{w}{\beta}\ \left(\frac{1}{\Gamma(\beta)}+t\right)^{\beta}+\Phi)}, \tag{3.25}$$

$$\mathcal{U}_{2.1.2} = h\ B_1\ \sqrt{\frac{2\ d_4}{d_2}}\ \cot\left[\left(\mathcal{T}\ x + \frac{\mathcal{L}}{\beta}\ \left(\frac{1}{\Gamma(\beta)} + t\right)^{\beta}\right)\ \sqrt{\frac{d_2}{2}}\right]\ e^{i(\gamma\ x + \frac{w}{\beta}\ \left(\frac{1}{\Gamma(\beta)}+t\right)^{\beta}+\Phi)}. \tag{3.26}$$

We can now obtain the exact solutions to Eqs. (1.1) and (1.2) based on the solution set (2.2), which is expressed as follows:

(2.2.1) The dark soliton solutions are obtained as follows if the following requirements are met $d_2 < 0$ and $d_4 > 0$:

$$\mathcal{P}_{2.2.1} = \alpha_1\sqrt{-\frac{d_2}{2d_4}}\ \tanh\left[\left(\mathcal{T}\ x + \frac{\mathcal{L}}{\beta}\ \left(\frac{1}{\Gamma(\beta)}+t\right)^{\beta}\right)\ \sqrt{-\frac{d_2}{2}}\right]\ e^{i(\gamma\ x+\frac{w}{\beta}\ \left(\frac{1}{\Gamma(\beta)}+t\right)^{\beta}+\Phi)}, \tag{3.27}$$

$$\mathcal{U}_{2.2.1} = h\ \alpha_1\sqrt{-\frac{d_2}{2d_4}}\ \tanh\left[\left(\mathcal{T}\ x + \frac{\mathcal{L}}{\beta}\ \left(\frac{1}{\Gamma(\beta)}+t\right)^{\beta}\right)\ \sqrt{-\frac{d_2}{2}}\right]\ e^{i(\gamma\ x+\frac{w}{\beta}\ \left(\frac{1}{\Gamma(\beta)}+t\right)^{\beta}+\Phi)}. \tag{3.28}$$

(2.2.2) The singular periodic solutions are obtained as follows if the following requirements are met $d_2 > 0$ and $d_4 > 0$:

$$\mathcal{P}_{2.2.2} = \alpha_1\sqrt{\frac{d_2}{2d_4}}\ \tan\left[\left(\mathcal{T}\ x + \frac{\mathcal{L}}{\beta}\ \left(\frac{1}{\Gamma(\beta)}+t\right)^{\beta}\right)\ \sqrt{\frac{d_2}{2}}\right]\ e^{i(\gamma\ x+\frac{w}{\beta}\ \left(\frac{1}{\Gamma(\beta)}+t\right)^{\beta}+\Phi)}, \tag{3.29}$$

$$\mathcal{U}_{2.2.2} = h\ \alpha_1\sqrt{\frac{d_2}{2d_4}}\ \tan\left[\left(\mathcal{T}\ x + \frac{\mathcal{L}}{\beta}\ \left(\frac{1}{\Gamma(\beta)}+t\right)^{\beta}\right)\ \sqrt{\frac{d_2}{2}}\right]\ e^{i(\gamma\ x+\frac{w}{\beta}\ \left(\frac{1}{\Gamma(\beta)}+t\right)^{\beta}+\Phi)}. \tag{3.30}$$

We can now obtain the exact solutions to Eqs. (1.1) and (1.2) based on the solution set (2.3), which is expressed as follows:

(2.3.1) The singular soliton solutions are obtained as follows if the following requirements are met $d_2 < 0$ and $d_4 > 0$:

$$\begin{aligned}\mathcal{P}_{2.3.1} =& 2B_1\sqrt{-\frac{2\ d_4}{d_2}}\ \operatorname{csch}\\ &\times\left[\left(\mathcal{T}\ x + \frac{\mathcal{L}}{\beta}\ \left(\frac{1}{\Gamma(\beta)}+t\right)^{\beta}\right)\ \sqrt{-2\ d_2}\right]\ e^{i(\gamma\ x+\frac{w}{\beta}\ \left(\frac{1}{\Gamma(\beta)}+t\right)^{\beta}+\Phi)},\end{aligned} \tag{3.31}$$

$$\begin{aligned}\mathcal{U}_{2.3.1} =& 2\ h\ B_1\sqrt{-\frac{2\ d_4}{d_2}}\ \operatorname{csch}\\ &\times\left[\left(\mathcal{T}\ x + \frac{\mathcal{L}}{\beta}\ \left(\frac{1}{\Gamma(\beta)}+t\right)^{\beta}\right)\ \sqrt{-2\ d_2}\right]\ e^{i(\gamma\ x+\frac{w}{\beta}\ \left(\frac{1}{\Gamma(\beta)}+t\right)^{\beta}+\Phi)}.\end{aligned} \tag{3.32}$$

(2.3.2) The singular periodic solutions are obtained as follows if the following requirements are met $d_2 > 0$ and $d_4 > 0$:

$$\mathcal{P}_{2.3.2} = 2B_1\sqrt{\frac{2\ d_4}{d_2}}\ \operatorname{csc}\left[\left(\mathcal{T}\ x + \frac{\mathcal{L}}{\beta}\ \left(\frac{1}{\Gamma(\beta)}+t\right)^{\beta}\right)\ \sqrt{2\ d_2}\right]\ e^{i(\gamma\ x+\frac{w}{\beta}\ \left(\frac{1}{\Gamma(\beta)}+t\right)^{\beta}+\Phi)}, \tag{3.33}$$

$$\mathcal{U}_{2.3.2} = 2\ h\ B_1\sqrt{\frac{2\ d_4}{d_2}}\ \operatorname{csc}\left[\left(\mathcal{T}\ x + \frac{\mathcal{L}}{\beta}\ \left(\frac{1}{\Gamma(\beta)}+t\right)^{\beta}\right)\ \sqrt{2\ d_2}\right]\ e^{i(\gamma\ x+\frac{w}{\beta}\ \left(\frac{1}{\Gamma(\beta)}+t\right)^{\beta}+\Phi)}. \tag{3.34}$$

Third situation: If the limitations $d_3 = d_4 = 0$ and $d_6 = 0$ are applied, we obtain a restricted set of solutions for the algebraic system, establishing a clear mathematical framework that yields limited results based on these conditions:

$$B_1 = 0,\ \alpha_1 = \tfrac{2\ \alpha_0\ d_2}{d_1},\ h = \mathcal{T}\left(\varepsilon(t)\left(2\ d_2\ \mathcal{T}^2\ \epsilon^2 + 3\gamma^2\ (r+1) - 3\gamma^3\ r\ \varepsilon(t) + 3r\ w\right) - 2\gamma\right).$$

Based on the previously given set of solutions, we can now obtain exact solutions for Eqs. (1.1) and (1.2) as follows:

(3.1) The hyperbolic solutions are obtained as follows if the following requirements are met $d_2 > 0$ and $d_0 = 0$:

$$\mathcal{P}_{3.1} = \alpha_0 \sinh\left[2\left(\mathcal{T}\ x + \frac{\mathcal{L}}{\beta}\ \left(\frac{1}{\Gamma(\beta)} + t\right)^{\beta}\right)\ \sqrt{d_2}\right]\ e^{i(\gamma\ x + \frac{w}{\beta}\ \left(\frac{1}{\Gamma(\beta)}+t\right)^{\beta} + \Phi)}, \tag{3.35}$$

$$\mathcal{U}_{3.1} = \alpha_0\ h\ \sinh\left[2\left(\mathcal{T}\ x + \frac{\mathcal{L}}{\beta}\ \left(\frac{1}{\Gamma(\beta)} + t\right)^{\beta}\right)\ \sqrt{d_2}\right]\ e^{i(\gamma\ x + \frac{w}{\beta}\ \left(\frac{1}{\Gamma(\beta)}+t\right)^{\beta} + \Phi)}. \tag{3.36}$$

(3.2) The periodic solutions are obtained as follows if the following requirements are met $d_2 < 0$ and $d_0 = 0$:

$$\mathcal{P}_{3.2} = \alpha_0 \sin\left[2\left(\mathcal{T}\ x + \frac{\mathcal{L}}{\beta}\ \left(\frac{1}{\Gamma(\beta)} + t\right)^{\beta}\right)\ \sqrt{-d_2}\right]\ e^{i(\gamma\ x + \frac{w}{\beta}\ \left(\frac{1}{\Gamma(\beta)}+t\right)^{\beta} + \Phi)}, \tag{3.37}$$

$$\mathcal{U}_{3.2} = \alpha_0\ h\ \sin\left[2\left(\mathcal{T}\ x + \frac{\mathcal{L}}{\beta}\ \left(\frac{1}{\Gamma(\beta)} + t\right)^{\beta}\right)\ \sqrt{-d_2}\right]\ e^{i(\gamma\ x + \frac{w}{\beta}\ \left(\frac{1}{\Gamma(\beta)}+t\right)^{\beta} + \Phi)}. \tag{3.38}$$

(3.3) The exponential solutions are obtained as follows if the following requirements are met $d_2 > 0$ and $d_0 = \frac{d_1^2}{4d_2}$:

$$\mathcal{P}_{3.3} = \frac{2\alpha_0 d_2}{d_1}\ e^{\left[i(\gamma\ x + \frac{w}{\beta}\ \left(\frac{1}{\Gamma(\beta)}+t\right)^{\beta} + \Phi) + \left(\mathcal{T}\ x + \frac{\mathcal{L}}{\beta}\ \left(\frac{1}{\Gamma(\beta)}+t\right)^{\beta}\right)\ \sqrt{d_2}\right]}, \tag{3.39}$$

$$\mathcal{U}_{3.2} = \frac{2\ \alpha_0\ d_2\ h}{d_1}\ e^{\left[i(\gamma\ x + \frac{w}{\beta}\ \left(\frac{1}{\Gamma(\beta)}+t\right)^{\beta} + \Phi) + \left(\mathcal{T}\ x + \frac{\mathcal{L}}{\beta}\ \left(\frac{1}{\Gamma(\beta)}+t\right)^{\beta}\right)\ \sqrt{d_2}\right]}. \tag{3.40}$$

Fourth situation: If the limitations $d_1 = d_3 = 0$ and $d_6 = 0$ are applied, we obtain a restricted set of solutions for the algebraic system, establishing a clear mathematical framework that yields limited results based on these conditions:

(4.1) $\alpha_1 = \alpha_1,\ \alpha_0 = \alpha_{-1} = 0,\ d_2 = \frac{-3\ \mathcal{T}\ \varepsilon(t)\left[\gamma^2 - r\ \gamma^3\ \varepsilon(t) + r\ \left(\gamma^2 + w\right)\right] + 2\gamma\ \mathcal{T} + \mathcal{L}}{2\mathcal{T}^3\ \varepsilon(t)}$.

(4.2) $B_1 = B_1,\ \alpha_0 = \alpha_1 = 0,\ d_2 = \frac{-3\ \mathcal{T}\ \varepsilon(t)\left[\gamma^2 - r\ \gamma^3\ \varepsilon(t) + r\ \left(\gamma^2 + w\right)\right] + 2\gamma\ \mathcal{T} + \mathcal{L}}{2\mathcal{T}^3\ \varepsilon(t)}$.

We can now obtain the exact solutions to Eqs. (1.1) and (1.2) based on the solution set (4.1), which is expressed as follows:

(4.1.1) The Jacobi elliptic solutions are obtained as follows if the following requirements are met $d_0 = \frac{d_2^2\ m^2\ \left(1-m^2\right)}{d_4\ \left(2m^2-1\right)^2}$, $d_2 > 0$, $d_4 < 0$ and $\frac{1}{\sqrt{2}} < m \leq 1$:

$$\mathcal{P}_{4.1.1} = m\ \ \alpha_1\ \sqrt{\frac{d_2}{d_4\ \left(1 - 2m^2\right)}}\ \ \mathrm{cn}$$

$$\times \left[\left(\mathcal{T}\ x+\frac{\mathcal{L}}{\beta}\ \left(\frac{1}{\Gamma(\beta)}+t\right)^{\beta}\right)\ \sqrt{\frac{d_2}{2\ m^2-1}}\right] e^{i(\gamma\ x+\frac{w}{\beta}\ \left(\frac{1}{\Gamma(\beta)}+t\right)^{\beta}+\Phi)}, \tag{3.41}$$

$$\mathcal{U}_{4.1.1} = h\ m\ \ \alpha_1\ \sqrt{\frac{d_2}{d_4\ (1-2m^2)}}\ \text{cn}$$
$$\times \left[\left(\mathcal{T}\ x+\frac{\mathcal{L}}{\beta}\ \left(\frac{1}{\Gamma(\beta)}+t\right)^{\beta}\right)\ \sqrt{\frac{d_2}{2\ m^2-1}}\right] e^{i(\gamma\ x+\frac{w}{\beta}\ \left(\frac{1}{\Gamma(\beta)}+t\right)^{\beta}+\Phi)}. \tag{3.42}$$

Eqs. (3.41) and (3.42) yield bright soliton solutions for $m = 1$ as follows:

$$\mathcal{P}_{4.1.3} = \alpha_1\ \sqrt{-\frac{d_2}{d_4}}\ \text{sech}\left[\left(\mathcal{T}\ x+\frac{\mathcal{L}}{\beta}\ \left(\frac{1}{\Gamma(\beta)}+t\right)^{\beta}\right)\ \sqrt{d_2}\right] e^{i(\gamma\ x+\frac{w}{\beta}\ \left(\frac{1}{\Gamma(\beta)}+t\right)^{\beta}+\Phi)}, \tag{3.43}$$

$$\mathcal{U}_{4.1.3} = h\ \alpha_1\ \sqrt{-\frac{d_2}{d_4}}\ \text{sech}\left[\left(\mathcal{T}\ x+\frac{\mathcal{L}}{\beta}\ \left(\frac{1}{\Gamma(\beta)}+t\right)^{\beta}\right)\ \sqrt{d_2}\right] e^{i(\gamma\ x+\frac{w}{\beta}\ \left(\frac{1}{\Gamma(\beta)}+t\right)^{\beta}+\Phi)}. \tag{3.44}$$

(4.1.2) The Jacobi elliptic solutions are obtained as follows if the following requirements are met $d_0 = \frac{d_2^2\ \left(1-m^2\right)}{d_4\ \left(2-m^2\right)^2}$, $d_2 > 0$, $d_4 < 0$ and $0 < m \leq 1$:

$$\mathcal{P}_{4.1.4} = \alpha_1\ \sqrt{\frac{m^2}{d_4\left(m^2-2\right)}}\ \text{dn}$$
$$\times \left[\left(\mathcal{T}\ x+\frac{\mathcal{L}}{\beta}\ \left(\frac{1}{\Gamma(\beta)}+t\right)^{\beta}\right)\ \sqrt{-\frac{d_2}{m^2-2}}\ \right] e^{i(\gamma\ x+\frac{w}{\beta}\ \left(\frac{1}{\Gamma(\beta)}+t\right)^{\beta}+\Phi)}, \tag{3.45}$$

$$\mathcal{U}_{4.1.4} = h\ \alpha_1\ \sqrt{\frac{m^2}{d_4\left(m^2-2\right)}}\ \text{dn}$$
$$\times \left[\left(\mathcal{T}\ x+\frac{\mathcal{L}}{\beta}\ \left(\frac{1}{\Gamma(\beta)}+t\right)^{\beta}\right)\ \sqrt{-\frac{d_2}{m^2-2}}\ \right] e^{i(\gamma\ x+\frac{w}{\beta}\ \left(\frac{1}{\Gamma(\beta)}+t\right)^{\beta}+\Phi)}. \tag{3.46}$$

Eqs. (3.45) and (3.46) yield bright soliton solutions for $m = 1$ as follows:

$$\mathcal{P}_{4.1.5} = \alpha_1\ \sqrt{-\frac{1}{d_4}}\ \text{sech}\left[\left(\mathcal{T}\ x+\frac{\mathcal{L}}{\beta}\ \left(\frac{1}{\Gamma(\beta)}+t\right)^{\beta}\right)\ \sqrt{d_2}\right] e^{i(\gamma\ x+\frac{w}{\beta}\ \left(\frac{1}{\Gamma(\beta)}+t\right)^{\beta}+\Phi)}, \tag{3.47}$$

$$\mathcal{U}_{4.1.5} = h\ \alpha_1\ \sqrt{-\frac{1}{d_4}}\ \text{sech}\left[\left(\mathcal{T}\ x+\frac{\mathcal{L}}{\beta}\ \left(\frac{1}{\Gamma(\beta)}+t\right)^{\beta}\right)\ \sqrt{d_2}\right] e^{i(\gamma\ x+\frac{w}{\beta}\ \left(\frac{1}{\Gamma(\beta)}+t\right)^{\beta}+\Phi)}. \tag{3.48}$$

(4.1.3) The Jacobi elliptic solutions are obtained as follows if the following requirements are met $d_0 = \frac{d_2^2\ m^2}{d_4\ \left(m^2+1\right)^2}$, $d_2 < 0$, $d_4 > 0$ and $0 < m \leq 1$:

$$\mathcal{P}_{6.1.6} = \alpha_1\ \sqrt{-\frac{d_2 m^2}{d_4\left(m^2+1\right)}}\ \text{sn}$$

$$\times \left[\left(\mathcal{T}\ x+\frac{\mathcal{L}}{\beta}\ \left(\frac{1}{\Gamma(\beta)}+t\right)^{\beta}\right)\ \sqrt{-\frac{d_2}{m^2+1}}\right] e^{i(\gamma\ x+\frac{w}{\beta}\ \left(\frac{1}{\Gamma(\beta)}+t\right)^{\beta}+\Phi)}, \tag{3.49}$$

$$\mathcal{U}_{6.1.6} = h\ \alpha_1\ \sqrt{-\frac{d_2 m^2}{d_4\,(m^2+1)}}\ \text{sn}$$
$$\times \left[\left(\mathcal{T}\ x+\frac{\mathcal{L}}{\beta}\ \left(\frac{1}{\Gamma(\beta)}+t\right)^{\beta}\right)\ \sqrt{-\frac{d_2}{m^2+1}}\right] e^{i(\gamma\ x+\frac{w}{\beta}\ \left(\frac{1}{\Gamma(\beta)}+t\right)^{\beta}+\Phi)}. \tag{3.50}$$

Eqs. (3.49) and (3.50) yield hyperbolic solutions for $m = 1$ as follows:

$$\mathcal{P}_{6.1.7} = \alpha_1\sqrt{-\frac{d_2}{d_4}}\tanh\left[\sqrt{\frac{-d_2}{2}}\ \left(\mathcal{T}x+\frac{\mathcal{L}}{\beta}\ \left[\frac{1}{\Gamma(\beta)}+t\right]^{\beta}\right)\right] e^{i(\gamma\ x+\frac{w}{\beta}\ \left(\frac{1}{\Gamma(\beta)}+t\right)^{\beta}+\Phi)}, \tag{3.51}$$

$$\mathcal{U}_{6.1.7} = h\ \alpha_1\sqrt{-\frac{d_2}{d_4}}\tanh\left[\sqrt{\frac{-d_2}{2}}\ \left(\mathcal{T}x+\frac{\mathcal{L}}{\beta}\ \left[\frac{1}{\Gamma(\beta)}+t\right]^{\beta}\right)\right] e^{i(\gamma\ x+\frac{w}{\beta}\ \left(\frac{1}{\Gamma(\beta)}+t\right)^{\beta}+\Phi)}. \tag{3.52}$$

We can now obtain the exact solutions to Eqs. (1.1) and (1.2) based on the solution set (4.2), which is expressed as follows:

(4.2.1) The Jacobi elliptic solutions are obtained as follows if the following requirements are met $d_0 = \frac{d_2^2\ m^2\ \left(1-m^2\right)}{d_4\ \left(2m^2-1\right)^2}$, $d_2 > 0$, $d_4 < 0$ and $\frac{1}{\sqrt{2}} < m \leq 1$:

$$\mathcal{P}_{4.2.1} = m\ B_1\ \sqrt{\frac{d_4\,(1-2m^2)}{d_2}}\ \text{nc}$$
$$\times \left[\left(\mathcal{T}\ x+\frac{\mathcal{L}}{\beta}\ \left(\frac{1}{\Gamma(\beta)}+t\right)^{\beta}\right)\ \sqrt{\frac{d_2}{2\ m^2-1}}\right] e^{i(\gamma\ x+\frac{w}{\beta}\ \left(\frac{1}{\Gamma(\beta)}+t\right)^{\beta}+\Phi)}, \tag{3.53}$$

$$\mathcal{U}_{4.2.1} = h\ m\ \ B_1\ \sqrt{\frac{d_4\,(1-2m^2)}{d_2}}\ \text{nc}$$
$$\times \left[\left(\mathcal{T}\ x+\frac{\mathcal{L}}{\beta}\ \left(\frac{1}{\Gamma(\beta)}+t\right)^{\beta}\right)\ \sqrt{\frac{d_2}{2\ m^2-1}}\right] e^{i(\gamma\ x+\frac{w}{\beta}\ \left(\frac{1}{\Gamma(\beta)}+t\right)^{\beta}+\Phi)}. \tag{3.54}$$

Eqs. (3.53) and (3.54) yield hyperbolic solutions for $m = 1$ as follows:

$$\mathcal{P}_{4.2.3} = B_1\ \cosh\sqrt{-\frac{d_4}{d_2}}\left[\left(\mathcal{T}\ x+\frac{\mathcal{L}}{\beta}\ \left(\frac{1}{\Gamma(\beta)}+t\right)^{\beta}\right)\ \sqrt{d_2}\right] e^{i(\gamma\ x+\frac{w}{\beta}\ \left(\frac{1}{\Gamma(\beta)}+t\right)^{\beta}+\Phi)}, \tag{3.55}$$

$$\mathcal{U}_{4.2.3} = h\ B_1\ \cosh\sqrt{-\frac{d_4}{d_2}}\left[\left(\mathcal{T}\ x+\frac{\mathcal{L}}{\beta}\ \left(\frac{1}{\Gamma(\beta)}+t\right)^{\beta}\right)\ \sqrt{d_2}\right] e^{i(\gamma\ x+\frac{w}{\beta}\ \left(\frac{1}{\Gamma(\beta)}+t\right)^{\beta}+\Phi)}. \tag{3.56}$$

(4.2.2) The Jacobi elliptic solutions are obtained as follows if the following requirements are met $d_0 = \frac{d_2^2\ \left(1-m^2\right)}{d_4\ \left(2-m^2\right)^2}$, $d_2 > 0$, $d_4 < 0$ and $0 < m \leq 1$:

$$\mathcal{P}_{4.2.4} = B_1\ \sqrt{\frac{d_4\,(m^2-2)}{m^2}}\ \text{nd}$$

$$\times \left[\left(\mathcal{T}\ x+\frac{\mathcal{L}}{\beta}\ \left(\frac{1}{\Gamma(\beta)}+t\right)^{\beta}\right)\ \sqrt{-\frac{d_2}{m^2-2}}\ \right] e^{i(\gamma\ x+\frac{w}{\beta}\ \left(\frac{1}{\Gamma(\beta)}+t\right)^{\beta}+\Phi)}, \tag{3.57}$$

$$\mathcal{U}_{4.2.4} = h\ B_1\ \sqrt{\frac{d_4\,(m^2-2)}{m^2}}\ \mathrm{nd}$$
$$\times \left[\left(\mathcal{T}\ x+\frac{\mathcal{L}}{\beta}\ \left(\frac{1}{\Gamma(\beta)}+t\right)^{\beta}\right)\ \sqrt{-\frac{d_2}{m^2-2}}\ \right] e^{i(\gamma\ x+\frac{w}{\beta}\ \left(\frac{1}{\Gamma(\beta)}+t\right)^{\beta}+\Phi)}. \tag{3.58}$$

Eqs. (3.57) and (3.58) yield hyperbolic solutions for $m = 1$ as follows:

$$\mathcal{P}_{4.2.5} = B_1\ \sqrt{-d_4}\ \cosh\left[\left(\mathcal{T}\ x+\frac{\mathcal{L}}{\beta}\ \left(\frac{1}{\Gamma(\beta)}+t\right)^{\beta}\right)\ \sqrt{d_2}\right] e^{i(\gamma\ x+\frac{w}{\beta}\ \left(\frac{1}{\Gamma(\beta)}+t\right)^{\beta}+\Phi)}, \tag{3.59}$$

$$\mathcal{U}_{4.2.4} = h\ B_1\ \sqrt{-d_4}\ \cosh\left[\left(\mathcal{T}\ x+\frac{\mathcal{L}}{\beta}\ \left(\frac{1}{\Gamma(\beta)}+t\right)^{\beta}\right)\ \sqrt{d_2}\right] e^{i(\gamma\ x+\frac{w}{\beta}\ \left(\frac{1}{\Gamma(\beta)}+t\right)^{\beta}+\Phi)}. \tag{3.60}$$

(4.2.3) The Jacobi elliptic solutions are obtained as follows if the following requirements are met $d_0 = \frac{d_2^2\ m^2}{d_4\ (m^2+1)^2}$, $d_2 < 0$, $d_4 > 0$ and $0 < m \leq 1$:

$$\mathcal{P}_{6.2.5} = B_1\ \sqrt{-\frac{d_4\ (m^2+1)}{d_2\ m^2}}\ \mathrm{ns}$$
$$\times \left[\left(\mathcal{T}\ x+\frac{\mathcal{L}}{\beta}\ \left(\frac{1}{\Gamma(\beta)}+t\right)^{\beta}\right)\ \sqrt{-\frac{d_2}{m^2+1}}\right] e^{i(\gamma\ x+\frac{w}{\beta}\ \left(\frac{1}{\Gamma(\beta)}+t\right)^{\beta}+\Phi)}, \tag{3.61}$$

$$\mathcal{U}_{6.2.5} = h\ B_1\ \sqrt{-\frac{d_4\ (m^2+1)}{d_2\ m^2}}\ \mathrm{ns}$$
$$\times \left[\left(\mathcal{T}\ x+\frac{\mathcal{L}}{\beta}\ \left(\frac{1}{\Gamma(\beta)}+t\right)^{\beta}\right)\ \sqrt{-\frac{d_2}{m^2+1}}\right] e^{i(\gamma\ x+\frac{w}{\beta}\ \left(\frac{1}{\Gamma(\beta)}+t\right)^{\beta}+\Phi)}. \tag{3.62}$$

Eqs. (3.61) and (3.62) yield hyperbolic solutions for $m = 1$ as follows:

$$\mathcal{P}_{6.2.6} = B_1\sqrt{-\frac{2d_4}{d_2}}\ \coth\left[\sqrt{\frac{-d_2}{2}}\ \left(\mathcal{T}x+\frac{\mathcal{L}}{\beta}\ \left[\frac{1}{\Gamma(\beta)}+t\right]^{\beta}\right)\right] e^{i(\gamma\ x+\frac{w}{\beta}\ \left(\frac{1}{\Gamma(\beta)}+t\right)^{\beta}+\Phi)}, \tag{3.63}$$

$$\mathcal{U}_{6.2.6} = h\ B_1\sqrt{-\frac{2d_4}{d_2}}\ \coth\left[\sqrt{\frac{-d_2}{2}}\ \left(\mathcal{T}x+\frac{\mathcal{L}}{\beta}\ \left[\frac{1}{\Gamma(\beta)}+t\right]^{\beta}\right)\right] e^{i(\gamma\ x+\frac{w}{\beta}\ \left(\frac{1}{\Gamma(\beta)}+t\right)^{\beta}+\Phi)}. \tag{3.64}$$

4. Physical applications of solitons in VCNLS equations with β-fractional derivatives

In this section, we present comprehensive graphical representations and detailed physical interpretations of the diverse solutions obtained for the variable-coefficient coupled nonlinear

Schrödinger (VCNLS) equations with β-fractional derivatives. Through systematic exploration of parameter spaces, we have identified numerous previously unrecorded solution families for Eqs. (1.1) and (1.2). This section features an extensive collection of 3-D and 2-D visualizations that elucidate the mathematical characteristics and physical behaviors of the discovered solutions. A crucial aspect of our analysis focuses on understanding the profound influence of the fractional order β and variable coefficients on soliton dynamics. The β-parameter fundamentally alters the wave dispersion and nonlinearity balance, leading to distinctive propagation characteristics not observed in integer-order models. Meanwhile, the time-dependent coefficients enable dynamic control over soliton evolution, mimicking realistic conditions in inhomogeneous media. Figure 1 Bright soliton solutions demonstrating the effect of fractional order β on pulse shaping of Eqs. (3.11) and (3.12), with parameters set to $d_4 = -0.45,\ d_2 = 2.5,\ \alpha_1 = 0.62,\ \mathcal{L} = 0.52,\ \mathcal{T} = -0.98,\ w = -0.63,\ \gamma = 0.72,\ \Phi = 0.69$, and $h = 2$. Figure 1 illustrates the bright soliton solutions of Eqs. (3.11) and (3.12). These localized intensity peaks represent self-trapped wave packets that maintain their shape through a balance between nonlinear self-focusing and fractional dispersion. The β-fractional derivative significantly influences the pulse sharpness and propagation stability, with lower β values exhibiting enhanced localization effects. The variable coefficient $\varepsilon(t)$ embedded in the transformation allows for controlled amplitude modulation, making these solutions particularly relevant for optical communication systems where signal shaping is crucial. Figure 2 illustrates the singular periodic solutions showing fractional-order induced modulation effects of Eqs. (3.13) and (3.14) with parameters $d_4 = 0.45,\ d_2 = -0.65,\ \alpha_1 = 0.62,\ \mathcal{L} = 0.52,\ \mathcal{T} = 0.8,\ w = 0.63,\ \gamma = 0.72,\ \Phi = 0.79$, and $h = 5$. Figure 2 illustrates the singular periodic solutions of Eqs. (3.13) and (3.14). These solutions exhibit characteristic periodic singularities that arise from the interplay between fractional dispersion and nonlinear coupling. The β parameter governs the singularity spacing and intensity, with distinct modulation patterns emerging at different fractional orders. Physically, such structures can model rogue wave phenomena in optical fibers or extreme events in plasma physics, where the variable coefficients account for environmental fluctuations inducing phase transitions between regular and singular behavior. Figure 3 illustrates the singular soliton solutions highlighting fractional derivative effects on singularity formation with parameters: $d_4 = 0.5,\ d_2 = -2.4,\ \alpha_1 = 0.64,\ \mathcal{L} = 0.62,\ \mathcal{T} = -0.94,\ w = -0.66,\ \gamma = 0.73,\ \Phi = 0.69$, and $h = 2$. Figure 3 illustrates the singular soliton solutions of Eqs. (3.23) and (3.24). These solutions feature narrow regions of extreme field enhancement, mathematically represented by singularities. The fractional order β critically determines the singularity strength and spatial confinement, with smaller β values leading to more pronounced singular behavior. In physical contexts, these solutions can describe optical field collapse in nonlinear media or charge accumulation in ferroelectric materials, where the variable coefficients model material inhomogeneities that either suppress or enhance singularity formation. These solutions are mainly defined by a narrow region that peaks at infinity. Figure 4 illustrates the dark soliton solution for Eqs. (3.27) and (3.28) with parameters $d_4 = 0.6,\ d_2 = -0.53,\ \alpha_1 = 0.7,\ \mathcal{L} = 0.8,\ \mathcal{T} = -0.84,\ w = -0.76,\ \gamma = 0.75,\ \Phi = 0.68$, and $h = 0.5$. Figure 4 illustrates the dark soliton solution for Eqs. (3.27) and (3.28). Dark solitons manifest as intensity dips in a continuous background, characterized by rapid phase jumps across the soliton core. The β-fractional derivative modifies the phase transition profile and soliton depth, enabling tunable notch filtering applications in photonic devices. The incorporation of variable coefficients through parameters $\mathcal{L}$ and $\mathcal{T}$ allows dynamic control over soliton velocity and interaction properties, facilitating their use in reconfigurable optical networks and Bose-Einstein condensate manipulation. Across all solution types, the fractional order β serves

as a crucial control parameter that continuously bridges classical and fractional dynamics. As $\beta \to 1$, we recover conventional integer-order behavior, while intermediate values exhibit hybrid characteristics with enhanced tunability. The variable coefficients provide additional degrees of freedom for adaptive soliton management in realistic environments with spatial or temporal inhomogeneities, significantly expanding the practical applicability of our findings in advanced photonic systems and nonlinear wave engineering.

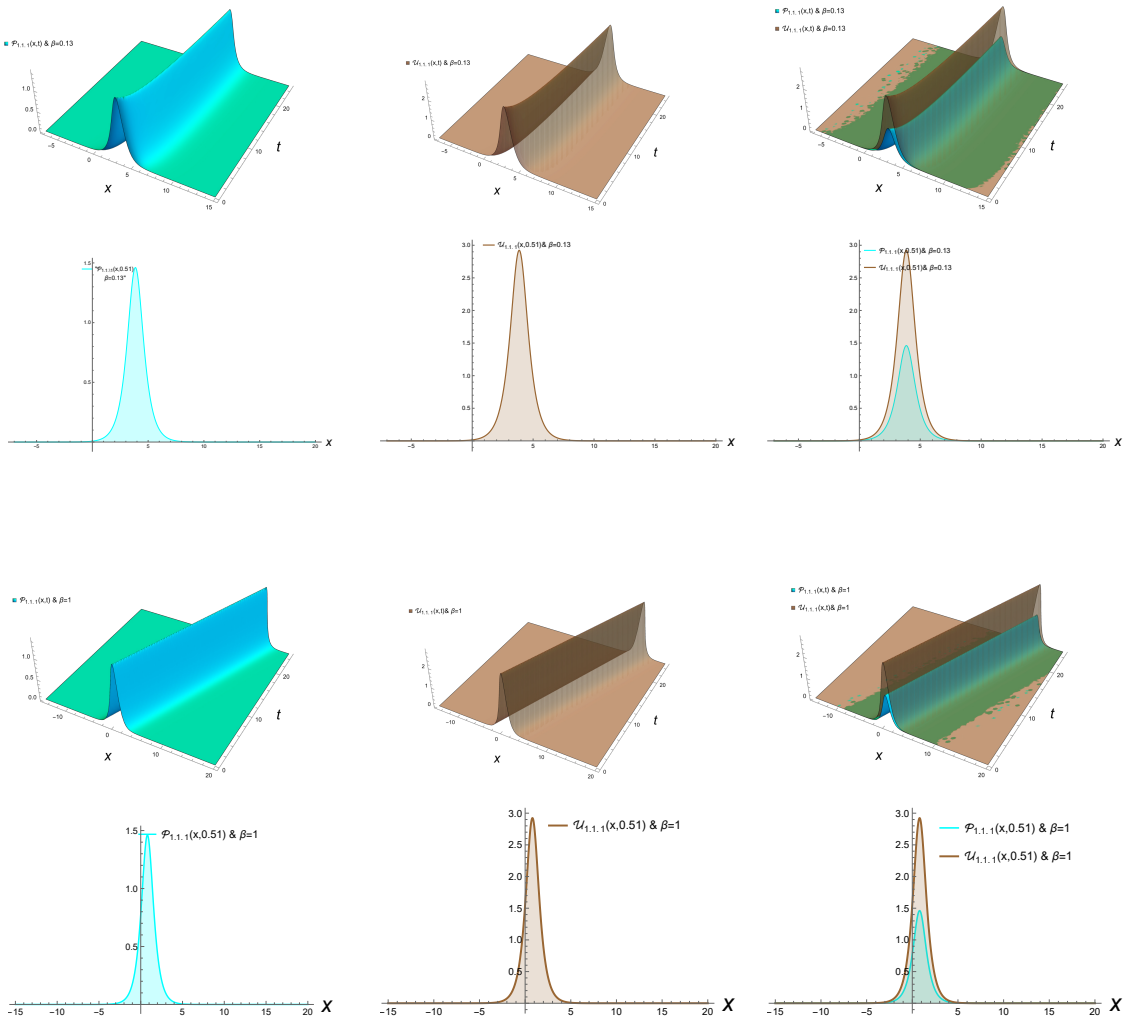

Figure 1. Diagrams in both two and three dimensions illustrate the bright soliton solutions obtained from Eqs. (3.11) and (3.12).

5. Results and discussion

The implementation of the IMETF method has yielded a rich variety of exact analytical solutions for the variable-coefficient coupled higher-order NLSE with β-fractional derivatives. Our investigation reveals several distinct classes of soliton solutions, each possessing unique mathematical characteristics and physical implications. The bright soliton solutions, exemplified by

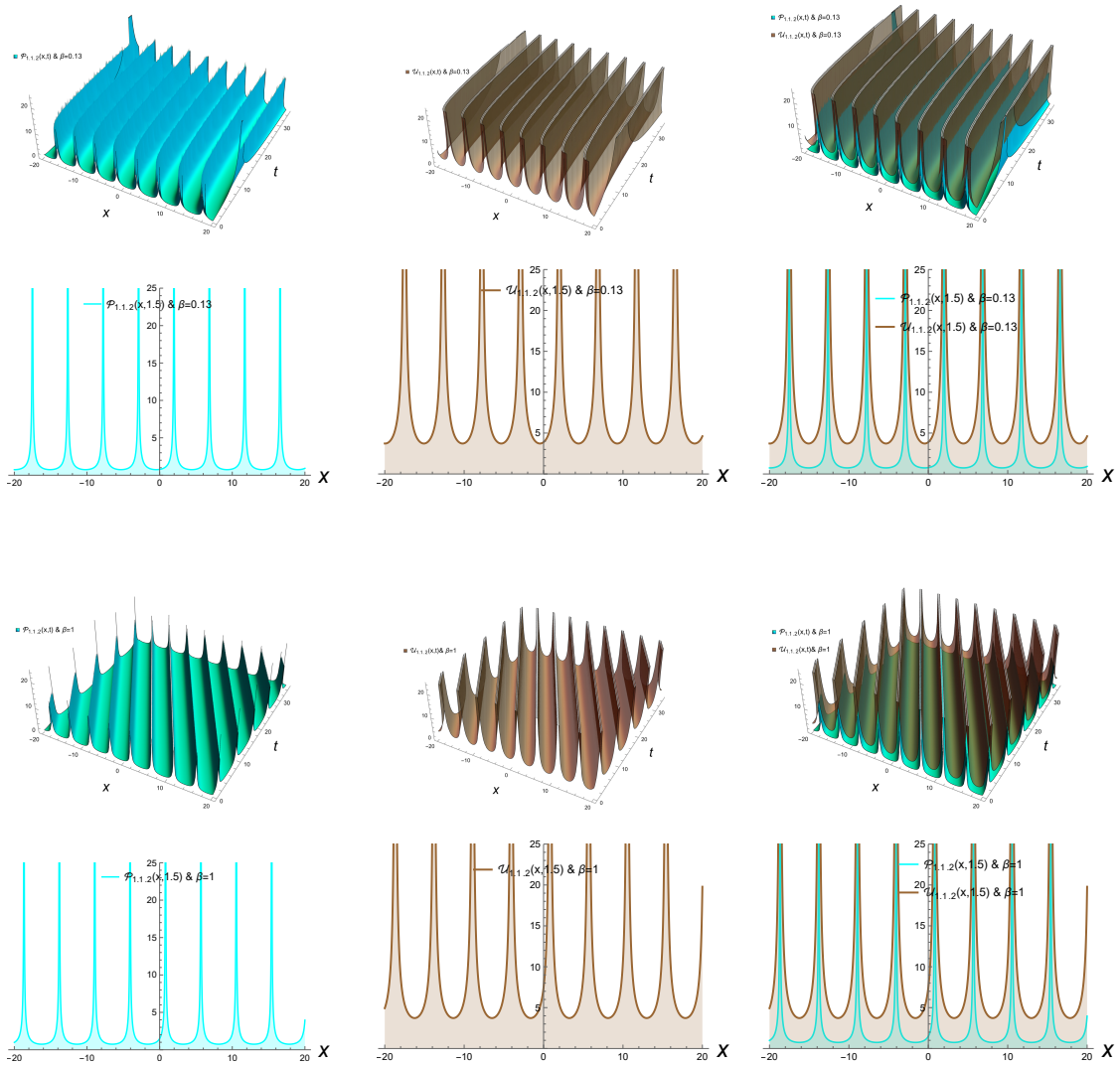

Figure 2. Diagrams in both two and three dimensions illustrate the singular periodic solutions obtained from Eqs. (3.13) and (3.14).

Eqs. (3.11) and (3.12), exhibit the characteristic sech-type profiles that maintain their shape and amplitude during propagation. These solutions demonstrate remarkable stability against perturbations, making them particularly suitable for optical communication applications where signal integrity is paramount. The intensity profiles show localized peaks with exponential decay, confirming their particle-like nature. Dark soliton solutions, as represented in Eqs. (3.27) and (3.28), manifest as intensity dips on a continuous background. These solutions are characterized by their topological stability and rapid phase shifts across the soliton core. The depth and width of these dark solitons can be precisely controlled through the variable coefficients, enabling tailored applications in optical filtering and signal processing. The fractional order parameter β emerges as a crucial factor governing soliton dynamics and characteristics. Our comparative analysis reveals several significant trends: As β decreases from the classical limit ($\beta = 1$) toward lower values ($\beta = 0.3$), we observe enhanced soliton localization and increased peak amplitudes.

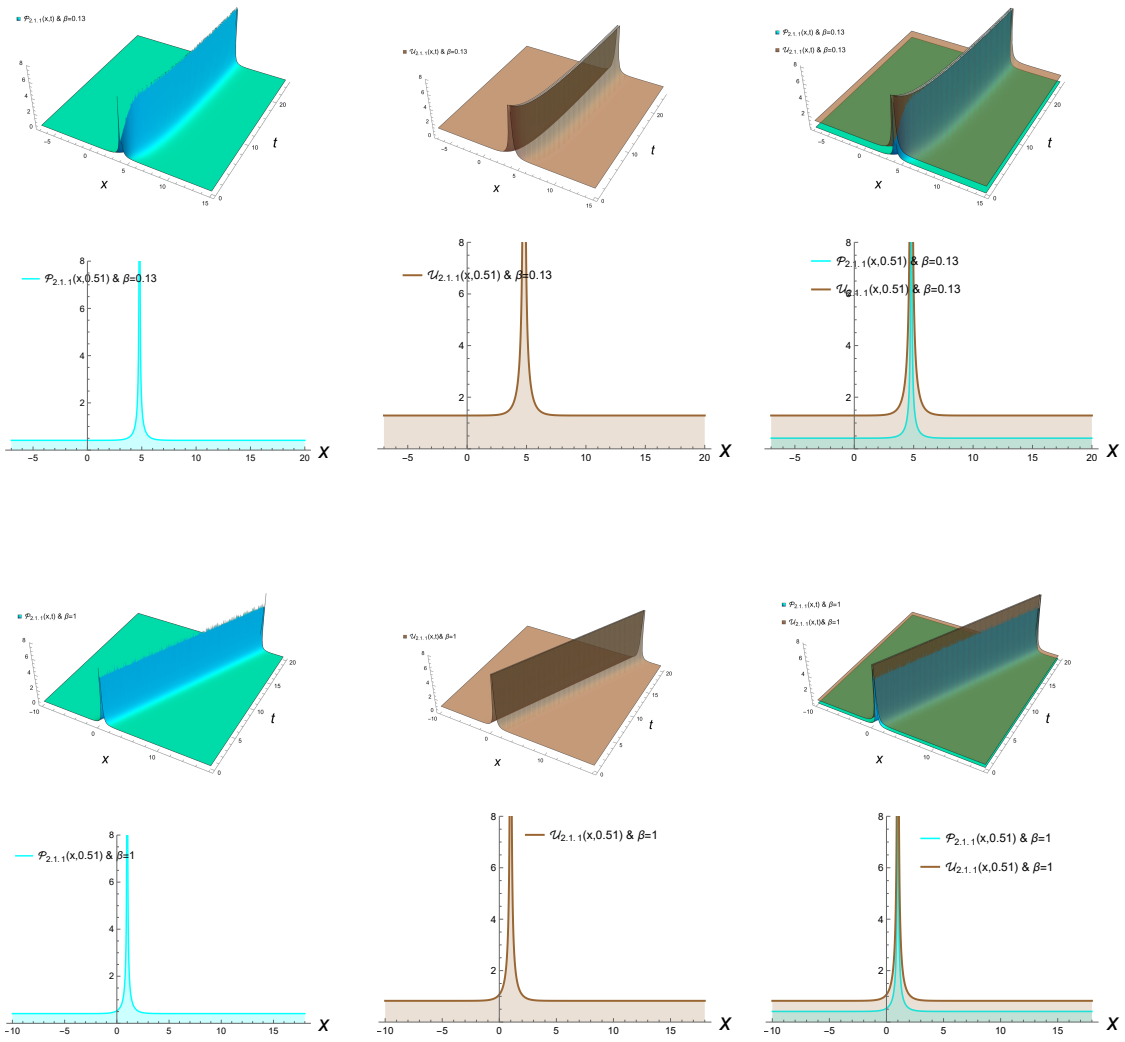

Figure 3. Diagrams in both two and three dimensions illustrate the singular soliton solutions obtained from Eqs. (3.23) and (3.24).

This amplification effect stems from the nonlocal nature of fractional derivatives, which introduces long-range interactions that reinforce soliton stability. The pulse width simultaneously decreases, leading to more compact soliton structures. The propagation characteristics also show strong β-dependence. Lower fractional orders result in reduced dispersion effects, allowing solitons to maintain their shape over longer propagation distances. This property is particularly advantageous for long-haul optical communication systems where signal degradation must be minimized. The time-dependent coefficients in our model provide unprecedented control over soliton dynamics. These variable parameters enable real-time adjustment of soliton properties, including: Amplitude modulation through coefficient variations allows dynamic signal amplification without changing the underlying physical system. This feature is crucial for adaptive optical networks where signal strength must be continuously optimized. Velocity control emerges as another significant advantage, with the variable coefficients directly influencing soliton propagation

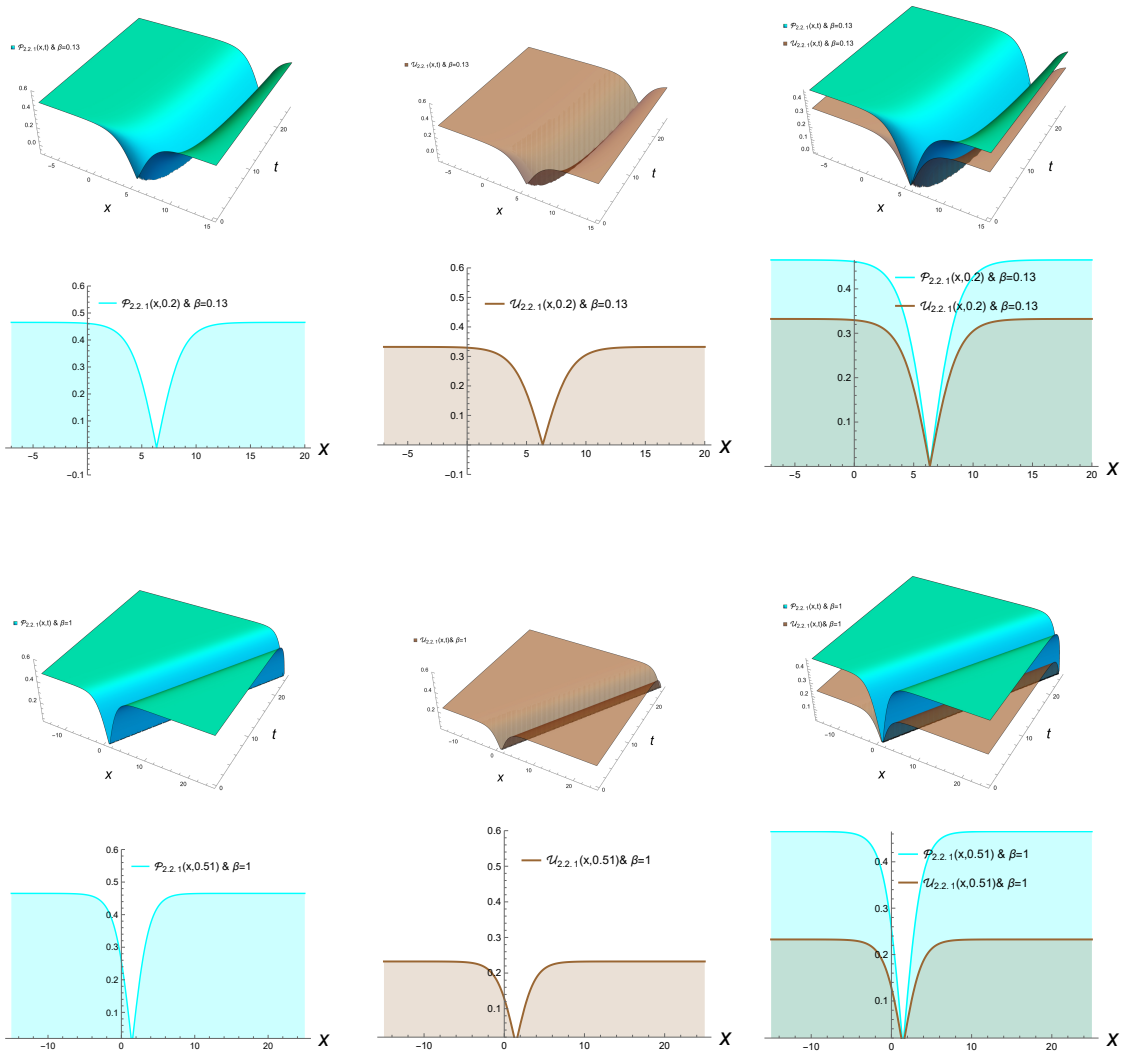

Figure 4. Diagrams in both two and three dimensions illustrate the dark soliton solutions obtained from Eqs. (3.27) and (3.28).

speed. This tunability facilitates precise temporal positioning of optical signals in communication applications. Interaction dynamics between coupled solitons can be manipulated through coordinated variation of multiple coefficients, enabling complex signal processing operations and interference management. The obtained solutions have profound implications for nonlinear optics and photonic technology. Bright solitons find immediate application in high-capacity optical communication systems, where their robustness and shape-preserving properties ensure reliable data transmission. The enhanced stability provided by fractional derivatives offers improved performance in noisy environments. Dark solitons show great promise for optical switching and logic operations, leveraging their phase discontinuity properties for information processing. The ability to dynamically control their characteristics through variable coefficients enables reconfigurable photonic circuits. Singular solutions provide valuable insights into extreme wave phenomena, contributing to our understanding of rogue waves in optical systems and facilitating the development of protective measures against such destructive events. The integration

of fractional calculus with variable-coefficient models represents a significant advancement in nonlinear wave theory, bridging the gap between idealized mathematical models and realistic physical systems with inherent inhomogeneities and memory effects.

6. Conclusions

This study has successfully implemented the Improved Modified Extended Tanh-Function (IMETF) method to investigate the dynamics of optical solitons in variable-coefficient coupled higher-order nonlinear Schrödinger equations (NLSEs) with β-fractional derivatives. Our work provides several significant advancements beyond previous research in this field: We have demonstrated that the incorporation of β-fractional derivatives introduces crucial nonlocal effects and memory-dependent properties that substantially alter soliton propagation characteristics. These fractional effects manifest as modified dispersion relations, enhanced nonlinear responses, and unique stabilisation mechanisms not observed in integer-order systems. The fractional order β serves as a powerful tuning parameter, enabling continuous control over soliton properties from classical to strongly nonlocal regimes. Our analysis reveals that as $\beta \to 1$, all obtained solutions smoothly converge to their classical counterparts, validating our methodology and establishing a coherent bridge between fractional and integer-order dynamics. This recovery of known results in the classical limit provides strong verification of our analytical approach while highlighting the extended capabilities of the fractional framework. The major outcomes of this research demonstrate that variable coefficients provide unprecedented control over soliton dynamics, enabling real-time adjustment of amplitude, width, velocity, and interaction properties. This tunability makes our model particularly valuable for practical applications in adaptive optical systems and reconfigurable photonic devices. For engineering applications, our results show significant potential in optical communications where robust solitons enable high-fidelity data transmission, and in photonic devices where variable coefficients allow dynamic control of soliton properties. The demonstrated ability to precisely manipulate soliton characteristics through fractional order parameters opens new avenues for technological innovation in signal processing and beyond. The research has uncovered a rich spectrum of soliton solutions, including: Stable bright solitons (Figure 1) exhibiting robust particle-like propagation. Dark solitons (Figure 4) demonstrate exceptional stability through intensity dips. Singular solitons (Figure 3) with complex amplitude structures. Singular periodic solutions, Jacobi elliptic function solutions, and various other wave structures. The effectiveness of the IMETF method in analyzing these complex fractional nonlinear systems provides both exact analytical solutions and fundamental insights into the physical mechanisms governing soliton behavior. This methodological approach offers a powerful framework for studying wave propagation in complex media with memory effects and inhomogeneities.

7. Future recommendations

For future research, several promising directions emerge extending this methodology to other fractional nonlinear systems, investigating soliton interactions and collision dynamics in greater detail, and exploring applications in emerging fields such as topological photonics and quantum information processing. The integration of variable coefficients with fractional calculus opens new possibilities for designing advanced photonic devices with tailored nonlinear responses and adaptive functionalities. This work establishes a comprehensive framework for soliton manage-

ment in fractional-order systems with variable parameters. The obtained results significantly expand our understanding of soliton behavior beyond conventional models and provide practical tools for developing advanced photonic technologies with enhanced functionality and adaptability in optical communications, signal processing, and related fields.

Acknowledgements

The authors would like to acknowledge the Deanship of Graduate Studies and Scientific Research, Taif University for funding this work.

References

[1] E. H. Abdullah, H. M. Ahmed, A. A. Zaghrout, A. I. A. Bahnasy and W. B. Rabie, *Effect of higher order on constructing the soliton waves to generalized nonlinear Schrödinger equation using improved modified extended tanh function method*, J. Optics, 2024, 1–11.

[2] E. H. Abdullah, H. M. Ahmed, A. A. Zaghrout, A. I. A. Bahnasy and W. B. Rabie, *Dynamical structures of optical solitons for highly dispersive perturbed NLSE with β-fractional derivatives and a sextic power-law refractive index using a novel approach*, Arabian J. Math., 2024, 1–14.

[3] M. A. Akbar, F. A. Abdullah, M. T. Islam, M. A. Al Sharif and M. S. Osman, *New solutions of the soliton type of shallow water waves and superconductivity models*, Results Phys., 2023, 44, 106180.

[4] N. Alessa, H. U. Rehman, S. Muneer and I. Iqbal, *Optical engineering perspectives on fractional analysis: A comprehensive study of the conformable Gross–Pitaevskii equation in the Bose–Einstein condensation*, Mod. Phys. Lett. B, 2025, 39(13), 2450491.

[5] M. H. Ali, H. M. El-Owaidy, H. M. Ahmed, A. A. El-Deeb and I. Samir, *Optical solitons and complexitons for generalized Schrödinger–Hirota model by the modified extended direct algebraic method*, Opt. Quantum Electron., 2023, 55(8), 675.

[6] G. Arora, R. Rani and H. Emadifar, *Soliton: A dispersion-less solution with existence and its types*, Heliyon, 2022, 8(12), 1–12.

[7] S. Boscolo, J. M. Dudley and C. Finot, *Solitons and coherent structures in optics: 50th anniversary of the prediction of optical solitons in fiber*, Opt. Commun., 2024, 131107.

[8] D. Chou, S. M. Boulaaras, H. U. Rehman, I. Iqbal and K. Khushi, *Fractional nonlinear doubly dispersive equations: Insights into wave propagation and chaotic behavior*, Alexandria Eng. J., 2025, 114, 507–525.

[9] D. Chou, I. Iqbal, A. F. Aljohani, S. Althobaiti and H. U. Rehman, *Exploring novel analytical methods for solving the heisenberg ferromagnetic-type fractional Akbota equation: Comparative graphical analysis*, Fractals, 2025, 33(8), 1–14.

[10] D. Chou, I. Iqbal, H. U. Rehman, O. H. Khalil and M. S. Osman, *Heat conduction dynamics: A study of lie symmetry, solitons, and modulation instability*, Rend. Lincei - Sci. Fis. Nat., 2025, 36(1), 315–336.

[11] J. M. Escorcia and E. Suazo, *On blow-up and explicit soliton solutions for coupled variable coefficient nonlinear Schrödinger equations*, Mathematics, 2024, 12(17), 2694.

[12] O. González-Gaxiola, Y. Yildirim, L. Hussein and A. Biswas, *Quiescent pure-quartic optical solitons with Kerr and non-local combo self-phase modulation by Laplace-Adomian decomposition*, J. Optics, 2024, 1–10.

[13] A. Hasegawa, *Soliton-based optical communications: An overview*, IEEE J. Sel. Top. Quantum Electron., 2002, 6(6), 1161–1172.

[14] A. Hasegawa, *New trends in optical soliton transmission systems: Proceedings of the symposium held in Kyoto, Japan*, Springer Science & Business Media, 2012, 5, 18–21.

[15] A. Hasegawa, *Optical soliton: Review of its discovery and applications in ultra-high-speed communications*, Front. Phys., 2022, 10, 1044845.

[16] M. F. Ismail, H. M. Ahmed and W. B. Rabie, *Construction of exact wave solutions for coupled thermoelasticity theory with temperature dependence using improved modified extended tanh-function method*, Contin. Mech. Thermodyn., 2025, 37(5), 77.

[17] A. J. A. M. Jawad, Y. Yildirim, A. Biswas and A. S. Alshomrani, *Optical solitons for the dispersive concatenation model with polarization mode dispersion by Sardar's sub-equation approach*, Contemp. Math., 2024, 1966–1989.

[18] L. Kaur and A. M. Wazwaz, *Bright–dark optical solitons for the Schrödinger-Hirota equation with variable coefficients*, Optik, 2019, 179, 479–484.

[19] A. Khalid, I. Haq, A. Rehan and M. S. Osman, *Developing and applying cubic spline method for the solution of boundary value problems in complex physical and engineering systems*, Partial Differ. Equ. Appl. Math., 2025, 101224.

[20] X. Liu, Q. Zhou, A. Biswas, A. K. Alzahrani and W. Liu, *The similarities and differences of different plane solitons controlled by (3+1)–dimensional coupled variable coefficient system*, J. Adv. Res., 2020, 24, 167–173.

[21] A. I. Maimistov, *Solitons in nonlinear optics*, Quantum Electron., 2010, 40(9), 756.

[22] N. Nasreen, A. R. Seadawy, D. Lu and M. Arshad, *Optical fibers to model pulses of ultrashort via generalized third-order nonlinear Schrödinger equation by using extended and modified rational expansion method*, J. Nonlinear Opt. Phys. Mater., 2024, 33(4), 2350058.

[23] K. S. Nisar, A. Ciancio, K. K. Ali, M. S. Osman, C. Cattani, D. Baleanu, A. Zafar, M. Raheel and M. Azeem, *On beta-time fractional biological population model with abundant solitary wave structures*, Alexandria Eng. J., 2022, 61(3), 1996–2008.

[24] W. B. Rabie and H. M. Ahmed, *Cubic-quartic solitons perturbation with couplers in optical metamaterials having triple-power law nonlinearity using extended F-expansion method*, Optik, 2022, 262, 169255.

[25] W. B. Rabie, H. M. Ahmed, M. Mirzazadeh, M. S. Hashemi and M. Bayram, *Retrieval solitons and other wave solutions to Kudryashov's equation with generalized anti-cubic nonlinearity and local fractional derivative using an efficient technique*, J. Optics, 2024, 1–9.

[26] H. U. Rehman, S. M. Boulaaras, M. A. El-Rahman, M. Umair Shahzad and D. Chou, *Exploring fluid behavior with space-time fractional-coupled Boussinesq equation*, Fractals, 2025, 33(4), 2540090.

[27] M. S. Saleem, S. Ahmad, Y. Alrashedi, T. Alrashdi and H. U. Rehman, *Fractional optical solitons in the coupled fokas system: White noise effects and sensitivity analysis*, Int. J. Mod. Phys. B, 2025, 39(25), 2550238.

[28] S. Sarker, G. S. Said, M. M. Tharwat, R. Karim, M. A. Akbar, N. S. Elazab, M. S. Osman and P. Dey, *Soliton solutions to a wave equation using the* (ϕ'/ϕ)*–expansion method*, Partial Differ. Equ. Appl. Math., 2023, 8, 100587.

[29] M. F. Shehab, H. M. Ahmed, S. Boulaaras, M. S. Osman and K. K. Ahmed, *Analyzing the impact of white noise on optical solitons and various wave solutions in the stochastic fourth-order nonlinear Schrödinger equation*, Alexandria Eng. J., 2025, 127, 1049–1063.

[30] S. Tarla, K. K. Ali, T. C. Sun, R. Yilmazer and M. S. Osman, *Nonlinear pulse propagation for novel optical solitons modeled by Fokas system in monomode optical fibers*, Results Phys., 2022, 36, 105381.

[31] H. Yi, X. Li, J. Zhang, X. Zhang and G. Ma, *Effective regulation of the interaction process among three optical solitons*, Chin. Phys. B, 2024, 33(10), 100502.

[32] U. Younas, J. Ren and M. Bilal, *Dynamics of optical pulses in fiber optics*, Mod. Phys. Lett. B, 2022, 36(5), 2150582.

Received July 2025; Accepted February 2026; Available online March 2026.